Theory of light scattering by longitudinal-acoustic phonons in superlattices

Jianjun He
Centre National d'Etudes des Télécommunications, 196 rue Henri Ravera, 92220 Bagneux, France

Bahram Djafari-Rouhani
Laboratoire de Physique du Solide, Faculté des Sciences et Techniques, Université de Haute Alsace, 4 rue des Frères Lumière, 68093 Mulhouse Cédex, France

Jacques Sapriel
Centre National d'Etudes des Télécommunications, 196 rue Henri Ravera, 92220 Bagneux, France
(Received 6 July 1987)

We study the scattering of light by longitudinal-acoustic phonons propagating along the axis of an infinite superlattice. In contrast to previous works, we take into account not only the difference between the acoustic and photoelastic parameters of the two media, but also the difference between their refractive indexes. In this case the incident and scattered light in the superlattice are represented by Bloch waves instead of plane waves. The scattering intensities, calculated in closed form by using a transfer-matrix method, are then valid for any value of the scattering wave vector q and not limited to q values small compared with the size of the Brillouin zone, π/D. The peak intensities are discussed for GaAs-AlAs superlattices as functions of the composition, period, and photoelastic parameters. The results may show noticeable differences with those of the previous works, especially for q near the boundaries of the successive Brillouin zones.

I. INTRODUCTION

A great deal of work has been devoted to light scattering from acoustic phonons, since the first observation of folded-longitudinal-acoustic modes (FLA) by Colvard *et al.*[1] Several experimental studies have been reported by Sapriel,[2] Colvard,[3] Jusserand,[4] and their collaborators in GaAs-$Ga_xAl_{1-x}As$ superlattices, and by Brugger,[5] Lockwood,[6] and their co-workers in Si-Ge_xSi_{1-x} superlattices. The peak frequency of the folded acoustic modes are well accounted for by both the elastic and linear chain models. Yet, the agreement between theory and experiment is less satisfactory when one considers the intensities of the acoustic modes (Brillouin line) and the FLA.

In Ref. 3, the distribution of scattered intensities in the FLA was considered as mainly due to the periodical square-wave modulation of the photoelastic constants in the superlattice, while the acoustic mismatch between GaAs and AlAs was totally neglected. Nevertheless this simple model led to analytical expressions for the intensities of the Brillouin line and the FLA modes, which can be considered as a correct first approach to the problem. One can still notice certain discrepancies with the experiments since the model of Ref. 3 yields intensities which are independent of the phonon wave vector and identical for the two components of the FLA doublets.

In a calculation by Babiker *et al.*[7] using a Green's-function method the modulation of the acoustic properties was taken into account but the superlattice was considered as a homogeneous medium with regard to the optic and photoelastic behavior. This model actually underestimates the intensities of the folded acoustic modes. Later Jusserand *et al.*[8] calculated these intensities numerically by including both the acoustic and photoelastic modulations; they solved the elasticity equation of motion by a Fourier series analysis and then obtained the intensities as the square modulus of the Fourier transform of the polarization. The asymmetry of the FLA doublets and the phonon wave-vector dependence of the intensity, observed in the experiments, were then accounted for by this model. Yet, no mention has been made of the unfolded acoustic modes in the superlattice. In addition, the optical mismatch between the two media was neglected, and the theoretical investigations of the intensities of the FLA were limited to scattering wave vectors $q=k_i \pm k_s$ less than the size of the Brillouin zone, π/D. Here k_i and k_s are the wave vectors of the incident and scattered lights and D is the period of the superlattice. The $\pm$ signs correspond, respectively, to backward and forward scattering.

We present here an improved calculation including, in addition to the elastic and photoelastic modulation, the difference between the refractive indexes of the materials. In this case, the incident and scattered lights are reflected back and forth at the multiple interfaces, thus giving rise to a complex interference phenomenon, which significantly modifies the intensity values for $q > \pi/D$, especially near the boundary of the successive Brillouin zones. The intensity of the scattered light is obtained in closed form, though its expression is rather complicated. Simpler analytic expressions are obtained in the particular cases which correspond to the simplifying assumptions of previous works.

A new setup combining the advantages of both Raman and Brillouin experiments has been constructed in the laboratory and allowed the investigation of modes whose frequency shift is as low as 1 cm^{-1}. Thus we were able to obtain the Brillouin line as well as the FLA on the same spectrum. The comparisons between the different peak intensities have been performed in good experimental conditions. Low-frequency phonons (<20 cm^{-1}) in GaAs-AlAs superlattices of period D larger than π/q have been investigated for the first time (the excitation wave vector now exceeds the Brillouin-zone edge π/D). The agreement between the experimental data on GaAs-AlAs superlattices and the novel theory of light scattering presented here will be examined in detail in the following paper.[9]

In the present study, the phonons in the acoustic range are treated as elastic waves propagating without attenuation in an infinite superlattice, with sharp and parallel interfaces between the layers; thus the modifications of the phonons due to the surface of the semi-infinite superlattice have been neglected. We only consider the longitudinal phonons propagating along the axis of the superlattice. Although we also neglect the absorption of the light, we assume that the polarization induced by the incident light extends over the N first unit cells of the superlattice from the surface; then we take the limit $N\to\infty$ at the end of the calculation. The intensity of the scattered light is obtained (Sec. II) for the backward scattering geometry, as in most of the experiments, but we also qualitatively discuss the forward scattering which is of interest for a superlattice bounded by air on both sides; this last situation is of practical interest since it can be obtained by removing the substrate (in the case of a GaAs-AlAs superlattice the substrate is GaAs, which is a particularly absorbing material) by chemical etching. We also discuss a few limiting cases of our general formula in which the superlattice behaves like an effective homogeneous medium for the propagation of optic and/or acoustic waves.

In Sec. III we present a few numerical applications of our results to the GaAs-AlAs superlattices which are experimentally the most studied systems. We investigate the sensitivity of the mode intensities to the chemical composition and to the ratio of the photoelastic constants of the materials.

II. LIGHT SCATTERING BY LONGITUDINAL-ACOUSTIC PHONONS

The superlattice is made of alternating layers of two different cubic crystals having their [001] direction along the axis of the superlattice. The period of the superlattice is $D=d_1+d_2$ where d_1 and d_2 are the thicknesses of the layers, respectively. We are interested in the scattering of light from longitudinal-acoustic phonons propagating along the x_3 axis; so we assume that all the electromagnetic waves (incident, scattered, and polarization waves) are polarized parallel to the x_1 axis and propagate along x_3. Under these assumptions, we can characterize each medium ($\mu=1,2$) in the superlattice by one elastic constant C_μ (which means C_{11}), the mass density ρ_μ, the dielectric constant $\epsilon_\mu=n_\mu^2$ (where n_μ is the index of refraction), and one photoelastic parameter $p_\mu=-\epsilon_\mu^2 p_{1133}^{(\mu)}$ (p_{1133} is the usual photoelastic constant we need in this calculation).

The coupling of the incident light to the phonons gives rise to a polarization in the superlattice through the photoelastic effect, which in turn creates the scattered field. Before dealing with this coupling mechanism, we briefly describe the necessary ingredients for the study of propagation of the acoustic and the electromagnetic waves in the superlattice; we use a transfer-matrix method which has been developed in detail in previous works.[10-12]

A. Longitudinal elastic waves in the superlattice

The equation of motion for a longitudinal elastic wave propagating along the axis of the superlattice (x_3 axis) is

$$\rho_\mu \frac{\partial^2 u_3(x_3,t)}{\partial t^2} - C_\mu \frac{\partial^2 u_3(x_3,t)}{\partial x_3^2} = 0 \tag{1}$$

in medium $\mu=1$ or 2. u_3 is the only nonzero component of the displacement field $\mathbf{u}(\mathbf{x},t)$. The solution of Eq. (1) takes the following general form:

$$u_3(n,\mu,x_3^{(n)};t) = (a_\mu^{(n)} e^{ik_{p\mu}x_3^{(n)}} + b_\mu^{(n)} e^{-ik_{p\mu}x_3^{(n)}}) e^{-i\omega_p t} , \tag{2}$$

where the subscript p refers to phonons, ω_p is the frequency of the phonon, and

$$k_{p\mu} = \frac{\omega_p}{v_\mu} \quad (\mu=1 \text{ or } 2) , \tag{3}$$

with $v_\mu=(C_\mu/\rho_\mu)^{1/2}$ the velocity of (longitudinal) sound in medium μ; the index n indicates the unit cell of the superlattice while $x_3^{(n)}$ is a local variable in each unit cell ranging from 0 to d_μ ($\mu=1$ or 2) in medium μ; the coefficients $a_\mu^{(n)}$ and $b_\mu^{(n)}$ are two multiplicative constants.

The solutions given by Eq. (2) are subject to the boundary conditions on the continuity of the displacement and of the normal stress at the consecutive interfaces. These relations may be written in matrix form at two successive interfaces as

$$\begin{bmatrix} 1 & 1 \\ 1 & -1 \end{bmatrix} \begin{bmatrix} a_2^{(n)} \\ b_2^{(n)} \end{bmatrix} = \begin{bmatrix} e^{ik_{p1}d_1} & e^{-ik_{p1}d_1} \\ \frac{1}{Z_p} e^{ik_{p1}d_1} & -\frac{1}{Z_p} e^{-ik_{p1}d_1} \end{bmatrix} \begin{bmatrix} a_1^{(n)} \\ b_1^{(n)} \end{bmatrix} \tag{4a}$$

and

$$\begin{bmatrix} 1 & 1 \\ 1 & -1 \end{bmatrix} \begin{bmatrix} a_1^{(n+1)} \\ b_1^{(n+1)} \end{bmatrix} = \begin{bmatrix} e^{ik_{p2}d_2} & e^{-ik_{p2}d_2} \\ Z_p e^{ik_{p2}d_2} & -Z_p e^{-ik_{p2}d_2} \end{bmatrix} \begin{bmatrix} a_2^{(n)} \\ b_2^{(n)} \end{bmatrix} \tag{4b}$$

with

$$Z_p = \frac{C_2 k_{p2}}{C_1 k_{p1}} = \frac{\rho_2 v_2}{\rho_1 v_1} . \tag{4c}$$

Combining Eqs. (4a) and (4b) one can relate the coefficients $a_1^{(n)}$ and $b_1^{(n)}$ in two successive unit cells

$$\begin{bmatrix} a_1^{(n+1)} \\ b_1^{(n+1)} \end{bmatrix} = \overleftrightarrow{T}_p \begin{bmatrix} a_1^{(n)} \\ b_1^{(n)} \end{bmatrix} , \tag{5}$$

where $\overleftrightarrow{T}_p$ is a 2×2 transfer matrix defined by

$$T_{p\,11} = T^*_{p\,22} = \left[\cos(k_{p2}d_2) + \frac{i}{2}\left[Z_p + \frac{1}{Z_p} \right] \sin(k_{p2}d_2) \right] e^{ik_{p1}d_1} , \tag{6a}$$

$$T_{p\,12} = T^*_{p\,21} = \frac{i}{2}\left[Z_p - \frac{1}{Z_p} \right] \sin(k_{p2}d_2) e^{-ik_{p1}d_1} . \tag{6b}$$

The determinant of the matrix $\overleftrightarrow{T}_p$ is equal to 1. In an infinite superlattice, one can also use the Bloch theorem

$$\begin{bmatrix} a_1^{(n+1)} \\ b_1^{(n+1)} \end{bmatrix} = e^{ik_pD} \begin{bmatrix} a_1^{(n)} \\ b_1^{(n)} \end{bmatrix} . \tag{7}$$

k_p is the wave vector associated to the phonon of frequency ω_p in the superlattice. Combining Eqs. (5) and (7), one obtains

$$(\overleftrightarrow{T}_p - e^{ik_pD}\overleftrightarrow{I}) \begin{bmatrix} a_1^{(n)} \\ b_1^{(n)} \end{bmatrix} = \begin{bmatrix} 0 \\ 0 \end{bmatrix} , \tag{8}$$

where $\overleftrightarrow{I}$ is a 2×2 unit matrix. The dispersion relation of the acoustic waves in the superlattice is then given by

$$\det(\overleftrightarrow{T}_p - e^{ik_pD}\overleftrightarrow{I}) = 0 , \tag{9a}$$

which can be written in the well-known form[13]

$$\cos(k_pD) = \cos(k_{p1}d_1)\cos(k_{p2}d_2) - \frac{1}{2}\left[Z_p + \frac{1}{Z_p} \right] \sin(k_{p1}d_1)\sin(k_{p2}d_2) . \tag{9b}$$

The dispersion curve is presented in Fig. 1 in an extended Brillouin-zone scheme for a GaAs-AlAs superlattice example. The following parameters have been used: $v_1 = 4726$ m/s, $v_2 = 5630$ m/s, $\rho_1 = 5.3149$, $\rho_2 = 3.745$, and $d_1/D = 0.26$, where the indices 1 and 2, respectively, refer to GaAs and AlAs; we have also used dimensionless wave vector and frequency

$$K = \frac{k_pD}{\pi}, \quad \Omega = \frac{\omega_pD}{2\pi c} , \tag{10}$$

where c is the velocity of the light in vacuum.

The curve in Fig. 1 can approximately be represented by a straight line whose equation is

$$\omega_p = V\,|\,k_p\,| , \tag{11}$$

where V is a mean acoustic velocity defined by

$$\frac{D}{V} = \frac{d_1}{v_1} + \frac{d_2}{v_2} . \tag{12}$$

This line approximately coincides with the true dispersion curve far from the boundaries of the Brillouin zones, and goes through the gaps at these boundaries. Let us also notice that the straight line becomes the true dispersion curve when there is no acoustic mismatch between the two materials, i.e., $\rho_1 v_1 = \rho_2 v_2$ or $Z_p = 1$

The solution of Eq. (8) can be written as

$$\begin{bmatrix} a_1^{(n)} \\ b_1^{(n)} \end{bmatrix} = U e^{ink_pD} \begin{bmatrix} 1 \\ \dfrac{e^{ik_pD} - T_{p\,11}}{T_{p\,12}} \end{bmatrix} , \tag{13a}$$

where U is a multiplicative factor and $\binom{a_2^{(n)}}{b_2^{(n)}}$ can be obtained from Eqs. (4a) and (13a):

$$\begin{bmatrix} a_2^{(n)} \\ b_2^{(n)} \end{bmatrix} = \frac{U}{2T_{p\,12}} e^{ink_pD} \begin{bmatrix} \left[1 - \dfrac{1}{Z_p}\right] (e^{i(k_pD - k_{p1}d_1)} - e^{-ik_{p2}d_2}) \\ \left[1 + \dfrac{1}{Z_p}\right] (e^{i(k_pD - k_{p1}d_1)} - e^{ik_{p2}d_2}) \end{bmatrix} . \tag{13b}$$

The only remaining unknown is the coefficient U, which can be deduced from the statistical energy associated to the phonon of frequency ω_p,

$$\int_{-\infty}^{+\infty} \rho(x_3)\omega_p^2\,|\,u_3(x_3,t)\,|^2 dx_3 \propto \hbar\omega_p\,|\,n(\omega_p) + \tfrac{1}{2}\,| , \tag{14}$$

where $n(\omega_p)$ is the Bose-Einstein distribution function. Using the Bloch wave character of u_3, the integration in Eq. (14) can be limited to only one period of the superlattice. In the following we also take the high-temperature limit ($kT \gg \hbar\omega_p$) of the Bose-Einstein distribution. Then Eq. (14) becomes

$$\sum_{\mu=1,2} \rho_\mu \left[(\,|\,a_\mu^{(0)}\,|^2 + |\,b_\mu^{(0)}\,|^2)D + \frac{i}{2k_{p\mu}}[a_\mu^{(0)*} b_\mu^{(0)}(1 - e^{2ik_{p\mu}d_\mu}) - a_\mu^{(0)} b_\mu^{(0)*}(1 - e^{-2ik_{p\mu}d_\mu})] \right] \propto \frac{kT}{\omega_p^2} , \tag{15}$$

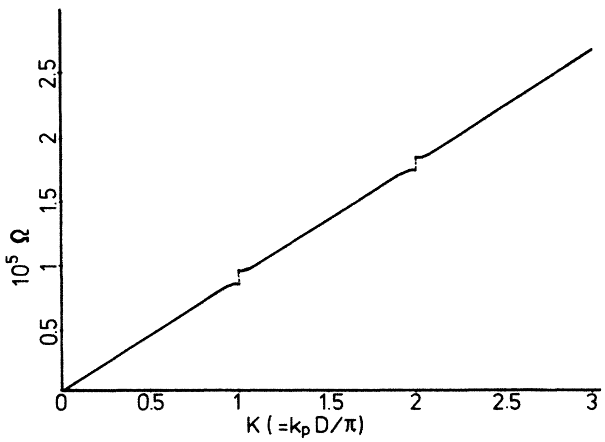

FIG. 1. Dispersion curve of the longitudinal-acoustic phonon in the extended Brillouin-zone scheme for a GaAs-AlAs superlattice.

from which one can obtain U.

B. Propagation of the incident light in the superlattice

The dispersion relation of an electromagnetic wave polarized parallel to the x_1 axis and propagating along the axis of the superlattice can also be obtained by the method presented in Sec. II A. Indeed, the Maxwell equations lead to the propagation equation

$$\frac{\partial^2 E(x_3,t)}{\partial x_3^2} - \frac{n_\mu^2}{c^2}\frac{\partial^2 E(x_3,t)}{\partial t^2} = 0 \qquad (16)$$

in medium $\mu=1$ or 2, where E stands for the x_1 component of the electric field. The general solution of Eq. (16) is

$$E(n,\mu,x_3^{(n)};t) = (A_\mu^{(n)} e^{ik_\mu x_3^{(n)}} + B_\mu^{(n)} e^{-ik_\mu x_3^{(n)}}) e^{-i\omega t} . \qquad (17)$$

Here c is the velocity of light in vacuum, ω the frequency, and

$$k_\mu = \frac{\omega n_\mu}{c} \quad (\mu=1 \text{ or } 2) . \qquad (18)$$

The magnetic field B associated to the electric field is parallel to the x_2 axis with

$$B(x_3,t) = -\frac{i}{\omega}\frac{\partial E(x_3,t)}{\partial x_3} . \qquad (19)$$

The boundary conditions at the interfaces on the continuity of E and B lead to equations similar to (4) with Z_p replaced by Z such that

$$Z = \frac{k_2}{k_1} = \frac{n_2}{n_1} . \qquad (20)$$

The transfer matrix $\overleftrightarrow{T}_p$ is then replaced by $\overleftrightarrow{T}$ such that

$$T_{11} = T_{22}^* = \left[\cos(k_2 d_2) + \frac{i}{2}\left[Z + \frac{1}{Z}\right]\sin(k_2 d_2)\right] e^{ik_1 d_1} ,$$

$$T_{12} = T_{21}^* = \frac{i}{2}\left[Z - \frac{1}{Z}\right]\sin(k_2 d_2) e^{-ik_1 d_1} . \qquad (21)$$

Finally the dispersion relation and the eigenvector associated to each wave can be deduced by transposition from Eqs. (7)–(9) and (13):

$$\cos(kD) = \cos(k_1 d_1)\cos(k_2 d_2) - \frac{1}{2}\left[Z + \frac{1}{Z}\right]\sin(k_1 d_1)\sin(k_2 d_2) , \qquad (22)$$

$$\begin{bmatrix} A_1^{(n)} \\ B_1^{(n)} \end{bmatrix} = E e^{iknD} \begin{bmatrix} 1 \\ \dfrac{e^{ikD} - T_{11}}{T_{12}} \end{bmatrix} , \qquad (23a)$$

$$\begin{bmatrix} A_2^{(n)} \\ B_2^{(n)} \end{bmatrix} = E\frac{e^{iknD}}{T_{12}} \times \begin{bmatrix} \dfrac{1}{2}\left[1 - \dfrac{1}{Z}\right](e^{i(kD - k_1 d_1)} - e^{-ik_2 d_2}) \\ \dfrac{1}{2}\left[1 + \dfrac{1}{Z}\right](e^{i(kD - k_1 d_1)} - e^{ik_2 d_2}) \end{bmatrix} . \qquad (23b)$$

Here k is the wave vector of the Bloch wave in the superlattice, which is also defined in the extended Brillouin-zone scheme as the phonon wave vector k_p.

In the following we shall use a subscript i or s in all the quantities appearing in Eqs. (16)–(23) (E, B, $A_\mu^{(n)}$, $B_\mu^{(n)}$, k_μ, k, ω, Z, $\overleftrightarrow{T}$) to refer to the incident electromagnetic field or to the scattered field (outside the polarized region). For a semi-infinite superlattice, the amplitude E in Eq. (20) can be related to the amplitude of the incident electric field in the vacuum, which can be written as

$$E(x_3,t) = \mathcal{E}_i e^{i(k_{i0} x_3 - \omega_i t)} \qquad (24)$$

with $k_{i0} = \omega_i / C$. Let us also assume that the free surface of the superlattice is at $x_3 = 0$ in medium $\mu=1$ in the unit cell $n=0$. Then the surface boundary conditions lead to

$$E_i = t_i \mathcal{E}_i \qquad (25a)$$

with the transmission coefficient t_i given by

$$t_i = \frac{2k_{i0} T_{i\,12}}{T_{i\,12}(k_{i0} + k_{i1}) + (e^{ik_i D} - T_{i\,11})(k_{i0} - k_{i1})} . \qquad (25b)$$

It is worthwhile to point out that the surface layer of the superlattice may have a composition or thickness different from those in the bulk; in this case some modifications arise in the transmission coefficient in (25b) as well as in the transmission of the scattered light from the superlattice into the vacuum. However, these modifications do not affect the scattering process, and as a consequence, do not play a role in the relative intensities of the folded acoustic modes at a given scattering wave vector.

C. Intensity of the scattered light

The propagation of an acoustic wave excites periodic variations of strain. In the presence of the incident electromagnetic wave, the photoelastic effect leads to a polarization of the superlattice along the x_1 axis whose anti-Stokes component is given by

$$P(x_3,t)=p_\mu \frac{\partial u_3(x_3,t)}{\partial x_3} E_i(x_3,t) \tag{26}$$

in medium μ. For Stokes polarization the $\partial u_3/\partial x_3$ factor should be replaced by $(\partial u_3/\partial x_3)^*$; however, the calculation of the scattered field will be similar in both cases. On the other hand, the factor $n(\omega_p)+\frac{1}{2}$ appearing in Eq. (14) should be replaced by $n(\omega_p)+1$ or $n(\omega_p)$ for Stokes or anti-Stokes polarization, respectively; this difference does not play a role in the high-temperature limit of Eq. (15).

We first assume that the superlattice is semi-infinite and the polarized domain extends from the unit cell $n=0$ at the surface up to the Nth unit cell. The radiation field generated by the polarization propagates out of the polarized region, into the vacuum on one side and inside the superlattice on the other side. The solution for the scattered field inside the polarized region should then be matched with a scattered Bloch wave propagating in the rest of the superlattice and with a scattered plane wave propagating in the vacuum far from the superlattice. However, one can overcome the effects of reflection and transmission of the waves at the surface of the superlattice by considering a more schematic situation where the radiation field propagates in an infinite superlattice on both sides of the polarized region.

Let us first obtain the general solution for the scattered field in the polarized domain. The knowledge of $u_3(x_3,t)$ and $E_i(x_3,t)$ enables one to write the (anti-Stokes) polarization in each film

$$P(n,\mu,x_3^{(n)};t)=ip_\mu k_{p\mu}(a_\mu^{(0)}e^{ik_{p\mu}x_3^{(n)}}-b_\mu^{(0)}e^{-ik_{p\mu}x_3^{(n)}})(A_{i\mu}^{(0)}e^{ik_{i\mu}x_3^{(n)}}+B_{i\mu}^{(0)}e^{-ik_{i\mu}x_3^{(n)}})e^{i(k_p+k_i)nD}e^{-i(\omega_p+\omega_i)t} . \tag{27}$$

In the presence of this polarization field, the Maxwell equations lead to the following equation for the scattered electric field $E_s(x_3,t)$:

$$\frac{\partial^2 E_s(x_3,t)}{\partial x_3^2}-\frac{n_\mu^2}{c^2}\frac{\partial^2 E_s(x_3,t)}{\partial t^2}=\frac{1}{\varepsilon_0 c^2}\frac{\partial^2 P(x_3,t)}{\partial t^2} \tag{28}$$

in medium μ, where ε_0 is the permittivity of the vacuum. The general solution in Eq. (28) contains two parts, a particular solution of the inhomogeneous equation and the general solution of the homogeneous equation. Defining the frequency ω_s of the scattered light as

$$\omega_s=\omega_i+\omega_p \tag{29}$$

and the wave vectors

$$k_{s\mu}=\frac{\omega_s}{c}n_\mu \quad (\mu=1,2) , \tag{30}$$

we obtain, in medium μ belonging to the cell n,

$$E_s(n,\mu,x_3^{(n)};t)=[M_\mu^{(n)}e^{ik_{s\mu}x_3^{(n)}}+N_\mu^{(n)}e^{-ik_{s\mu}x_3^{(n)}}+S_\mu(x_3^{(n)})e^{in(k_i+k_p)D}E_i]e^{-i\omega_s t} . \tag{31}$$

The $S_\mu(x_3^{(n)})$ which define the particular solution may be written

$$S_\mu(x_3^{(n)})=\frac{p_\mu k_{p\mu}\omega_s^2}{i\varepsilon_0 c^2 E_i}\left\{\frac{a_\mu^{(0)}A_{i\mu}^{(0)}e^{i(k_{p\mu}+k_{i\mu})x_3^{(n)}}-b_\mu^{(0)}B_{i\mu}^{(0)}e^{-i(k_{p\mu}+k_{i\mu})x_3^{(n)}}}{k_{s\mu}^2-(k_{p\mu}+k_{i\mu})^2}+\frac{a_\mu^{(0)}B_{i\mu}^{(0)}e^{i(k_{p\mu}-k_{i\mu})x_3^{(n)}}-b_\mu^{(0)}A_{i\mu}^{(0)}e^{-i(k_{p\mu}-k_{i\mu})x_3^{(n)}}}{k_{s\mu}^2-(k_{p\mu}-k_{i\mu})^2}\right\}, \quad \mu=1,2 . \tag{32}$$

Every quantity is known in Eq. (32). The magnetic field B in each medium can be deduced from Eq. (19); it contains the derivatives $S'_\mu(x_3)$ of $S_\mu(x_3)$. Using the continuity conditions of E and B at the interfaces, one can relate the fields in two successive cells in the same way as in Sec. II B:

$$\begin{bmatrix} M_1^{(n+1)} \\ N_1^{(n+1)} \end{bmatrix}=\overleftrightarrow{T}_s \begin{bmatrix} M_1^{(n)} \\ N_1^{(n)} \end{bmatrix}+\begin{bmatrix} W \\ V \end{bmatrix}e^{in(k_p+k_i)D} . \tag{33}$$

In Eq. (33) the elements of the transfer matrix $\overleftrightarrow{\mathrm{T}}_s$ are given by Eqs. (21) where a subscript s should be added to each quantity; the last term $\binom{W}{V}$ is due to the polarization field and may be written as a function of $S_\mu(0)$, $S_\mu(d_\mu)$, and also $S'_\mu(0)$ and $S'_\mu(d_\mu)$ ($\mu=1$ and 2):

$$\begin{bmatrix} W \\ V \end{bmatrix} = \frac{1}{2}\begin{bmatrix} 1 & 1 \\ 1 & -1 \end{bmatrix}\begin{bmatrix} S_2(d_2)-S_1(0)e^{i(k_p+k_i)D} \\ -\frac{i}{k_{s_1}}[S'_2(d_2)-S'_1(0)e^{i(k_p+k_i)D}] \end{bmatrix} + \frac{1}{2}\begin{bmatrix} \cos(k_{s2}d_2)+iZ_s\sin(k_{s2}d_2) & i\sin(k_{s2}d_2)+Z_s\cos(k_{s2}d_2) \\ \cos(k_{s2}d_2)-iZ_s\sin(k_{s2}d_2) & i\sin(k_{s2}d_2)-Z_s\cos(k_{s2}d_2) \end{bmatrix}\begin{bmatrix} S_1(d_1)-S_2(0) \\ \frac{-i}{k_{s2}}[S'_1(d_1)-S'_2(0)] \end{bmatrix} . \tag{34}$$

By repeating Eq. (33) several times one can relate the scattered field in the utmost layers of the polarized domain in the superlattice, i.e., the layers $n=0$ and $n=N$. It is convenient to define the matrix $\overleftrightarrow{\mathrm{Q}}$ which diagonalizes the transfer matrix $\overleftrightarrow{\mathrm{T}}_s$; calling e^{ik_sD} and e^{-ik_sD} the two eigenvalues of the matrix $\overleftrightarrow{\mathrm{T}}_s$ [k_s is defined by Eq. (22)], one has

$$\overleftrightarrow{\mathrm{Q}} = \begin{bmatrix} 1 & \dfrac{T_{s\,12}}{e^{-ik_sD}-T_{s\,11}} \\ \dfrac{e^{ik_sD}-T_{s\,11}}{T_{s\,12}} & 1 \end{bmatrix} \tag{35}$$

and

$$\overleftrightarrow{\mathrm{Q}}^{-1}\overleftrightarrow{\mathrm{T}}_s\overleftrightarrow{\mathrm{Q}} = \begin{bmatrix} e^{ik_sD} & 0 \\ 0 & e^{-ik_sD} \end{bmatrix} . \tag{36}$$

Then Eq. (33) leads to

$$\begin{bmatrix} M_1^{(N)} \\ N_1^{(N)} \end{bmatrix} = \overleftrightarrow{\mathrm{Q}}\begin{bmatrix} e^{iNk_sD} & 0 \\ 0 & e^{-iNk_sD} \end{bmatrix}\overleftrightarrow{\mathrm{Q}}^{-1}\begin{bmatrix} M_1^{(0)} \\ N_1^{(0)} \end{bmatrix} + \overleftrightarrow{\mathrm{Q}}\begin{bmatrix} \dfrac{e^{iN(k_p+k_i)D}-e^{iNk_sD}}{e^{i(k_p+k_i)D}-e^{ik_sD}} & 0 \\ 0 & \dfrac{e^{iN(k_p+k_i)D}-e^{-iNk_sD}}{e^{i(k_p+k_i)D}-e^{-ik_sD}} \end{bmatrix}\overleftrightarrow{\mathrm{Q}}^{-1}\begin{bmatrix} W \\ V \end{bmatrix} , \tag{37}$$

i.e., a relation between the column vectors $\binom{M_1^{(N)}}{N_1^{(N)}}$ and $\binom{M_1^{(0)}}{N_1^{(0)}}$.

Let us now introduce the scattered field outside the domain of polarization. In the vacuum side this is a plane wave whose electric field may be written

$$E(x_3,t)=\mathcal{E}_s e^{-i(k_{s0}x_3+\omega_s t)} \tag{38}$$

with

$$k_{s0}=\frac{\omega_s}{c} . \tag{39}$$

The boundary conditions at the surface of the superlattice relate the column vector $\binom{M_1^{(0)}}{N_1^{(0)}}$ to $\mathcal{E}_s$. Beyond the Nth unit cell in the superlattice, one can write the electric field of the scattered light like a Bloch wave as in Eq. (17):

$$E(n,\mu,x_3^{(n)};t)=(A_{s\mu}e^{ik_{s\mu}x_3^{(n)}}+B_{s\mu}e^{-ik_{s\mu}x_3^{(n)}})e^{i(nk_sD-\omega_s t)} . \tag{40}$$

With these notations the wave vectors k_s are assumed to be positive, just as k_i.

We recall that the coefficients $A_{s\mu}$ and $B_{s\mu}$ are known quantities [Eqs. (23)] except for a multiplicative factor E_s as in Eqs. (23). Let us assume that the transition from the nonpolarized to polarized region in the superlattice takes place at the abscissa $x_3^{(N)}=0$ in the medium $\mu=1$ of the unit cell N. At this position there are continuity conditions between the solutions on both sides given, respectively, by Eqs. (31) and (40). This relates the column vector $\binom{M_1^{(N)}}{N_1^{(N)}}$ to E_s.

In a final stage one can eliminate in Eq. (37) the column vectors $\binom{M_1^{(N)}}{N_1^{(N)}}$ and $\binom{M_1^{(0)}}{N_1^{(0)}}$ as functions, respectively, of E_s and $\mathcal{E}_s$; then, we are led to two equations with two unknowns E_s and $\mathcal{E}_s$ which become, after some algebra,

$$e^{iNk_sD}E_s\begin{bmatrix}1\\0\end{bmatrix}-\tfrac{1}{2}\mathcal{E}_s\begin{bmatrix}e^{iNk_sD} & 0\\ 0 & e^{-iNk_sD}\end{bmatrix}\overleftrightarrow{Q}^{-1}\begin{bmatrix}1 & -1\\ 1 & 1\end{bmatrix}\begin{bmatrix}1\\ \dfrac{k_{s0}}{k_{s1}}\end{bmatrix}$$

$$=E_i\begin{bmatrix}\dfrac{e^{iN(k_p+k_i)D}-e^{iNk_sD}}{e^{i(k_p+k_i)D}-e^{ik_sD}} & 0\\ 0 & \dfrac{e^{iN(k_p+k_i)D}-e^{-iNk_sD}}{e^{i(k_p+k_i)D}-e^{-ik_sD}}\end{bmatrix}\overleftrightarrow{Q}^{-1}\begin{bmatrix}W\\V\end{bmatrix}+E_i\begin{bmatrix}X\\Y\end{bmatrix} \quad (41)$$

with

$$\begin{bmatrix}X\\Y\end{bmatrix}=\frac{1}{2}\begin{bmatrix}e^{iN(k_p+k_i)D}-e^{iNk_sD} & 0\\ 0 & e^{iN(k_p+k_i)D}-e^{-iNk_sD}\end{bmatrix}\overleftrightarrow{Q}^{-1}\begin{bmatrix}1 & -1\\ 1 & 1\end{bmatrix}\begin{bmatrix}S_1(0)\\ \dfrac{i}{k_{s1}}S_1'(0)\end{bmatrix}. \quad (42)$$

In the right-hand side of Eq. (41), the first term contains the effect of the polarization of N unit cells in the superlattice, whereas the second term $\binom{X}{Y}$ is only related to the utmost polarized layers. When the number N goes to infinity, the latter term can be neglected with respect to the former and the calculation will be simplified; indeed, remembering that

$$\lim_{N\to\infty}\frac{|e^{iNx}-1|^2}{x^2}=2\pi N\delta(x)\ , \quad (43)$$

one can see that the first term in Eq. (41) contributes to the intensity of the scattered light by factors of the form $N\delta(k_p+k_i\pm k_s+2\pi m/D)$, where m is any integer, while the term $\binom{X}{Y}$ does not give any contribution proportional to N. Then, defining

$$\Delta k_\pm=k_p+k_i\pm k_s \quad (44)$$

and taking the limit $N\to\infty$, we obtain the amplitudes of the scattered fields

$$\frac{\mathcal{E}_s}{E_i}=-e^{ik_sD}t_s\frac{e^{iN\Delta k_+D}-1}{e^{i\Delta k_+D}-1}v\ , \quad (45a)$$

$$\frac{E_s}{E_i}=e^{-ik_sD}\frac{e^{iN\Delta k_-D}-1}{e^{i\Delta k_-D}-1}w+e^{ik_sD}r_s\frac{e^{iN\Delta k_+D}-1}{e^{i\Delta k_+D}-1}v\ , \quad (45b)$$

where

$$\begin{bmatrix}w\\v\end{bmatrix}=\overleftrightarrow{Q}^{-1}\begin{bmatrix}W\\V\end{bmatrix} \quad (46a)$$

and

$$t_s=\frac{e^{-ik_sD}-e^{ik_sD}}{e^{-ik_sD}-T_{s\,11}}\,\frac{2k_{s1}T_{s\,12}}{T_{s\,12}(k_{s0}+k_{s1})+(e^{ik_sD}-T_{s\,11})(k_{s0}-k_{s1})}\ , \quad (46b)$$

$$r_s=-\frac{T_{s\,12}}{e^{-ik_sD}-T_{s\,11}}\,\frac{T_{s\,12}(k_{s0}+k_{s1})+(e^{-ik_sD}-T_{s\,11})(k_{s0}-k_{s1})}{T_{s\,12}(k_{s0}+k_{s1})+(e^{ik_sD}-T_{s\,11})(k_{s0}-k_{s1})}\ , \quad (46c)$$

and t_s and r_s are, respectively, the coefficients of transmission and reflection of a Bloch wave at the surface of the superlattice. In the limit $n_1=n_2$, these results become

$$t_s=\frac{2k_{s1}}{k_{s0}+k_{s1}},\quad r_s=\frac{k_{s1}-k_{s0}}{k_{s0}+k_{s1}}\ ,$$

which are the well-known transmission and reflection coefficients for a plane wave.

Let us recall that in Eqs. (45) and (46) giving the expressions of the scattered fields, $\overleftrightarrow{T}_s$, $\overleftrightarrow{Q}$, and $\binom{W}{V}$, are, respectively, defined in Eqs. (21), (35), and (34), the indices i and s refer to the incident and scattered lights; k_{i0} and k_{s0} are the wave vectors of the plane waves associated to the incident and scattered lights in the vacuum, k_i and k_s the corresponding wave vectors of the Bloch waves in the superlattice (with our notations all these wave vectors are positive); $k_{s1}=(\omega_s/c)n_1$; and k_p is the wave vector of the phonon in the superlattice. Let us also notice that k_s, k_i, and k_p are defined in the extended Brillouin-zone scheme.

Instead of Eq. (45a) it would be more interesting to compare $\mathcal{E}_s$ to the amplitude $\mathcal{E}_i$ of the incident light in the vacuum. Using Eq. (25a) in (45a)

$$\frac{\mathcal{E}_s}{\mathcal{E}_i}=t_i t_s e^{ik_s D}\frac{e^{iN\Delta k_+ D}-1}{e^{i\Delta k_+ D}-1}v \; . \tag{47}$$

Thus the relative intensity of the backward scattered light becomes

$$I=\left|\frac{\mathcal{E}_s}{\mathcal{E}_i}\right|^2=\frac{\sin^2(N\,\Delta k_+ D/2)}{\sin^2(\Delta k_+ D/2)}\,|\,t_i t_s v\,|^2 \; . \tag{48}$$

In the limit $N\rightarrow\infty$, one obtains the wave-vector selection rule

$$k_p+k_i+k_s+\frac{2\pi m}{D}=0 \; , \tag{49a}$$

where m is an integer.

We see that, for a given scattering wave vector q $(=k_i+k_s)$, a series of phonon modes are excited. The frequencies of the excited phonon modes are determined by Eq. (49a) and the dispersion relation (9b). Figure 2 shows the frequencies of the lowest modes for q ranging from 0 to $3\pi/D$. Actually it is obtained by folding the dispersion curve (Fig. 1) into the successive Brillouin zones. The LA is the direct longitudinal-acoustic model (Brillouin line), corresponding to $m=0$. The folded acoustic modes corresponding to $m\neq 0$ are labeled as $(\mathrm{FLA})_m$. It is worthwhile pointing out that the frequencies of certain folded modes can be lower than the Brillouin mode when the scattering wave vector exceeds the first Brillouin zone. This occurs with long-period superlattices as investigated in Ref. 9.

In the forward scattering, Eq. (45b) shows that, in addition to the peaks corresponding to Eq. (49a), one can also observe the folded acoustic modes at the phonon wave vector satisfying

$$k_p+k_i-k_s+\frac{2\pi m}{D}=0 \; . \tag{49b}$$

In the above formulas, we distinguished between the frequencies of the incident and the scattered fields. However, in general, the frequency of the phonon is much smaller than those of the lights; $\omega_p \ll \omega_i$ or ω_s. So, one can assume instead of (29)

$$\omega_i \simeq \omega_s \tag{50a}$$

and as a consequence

$$k_i \simeq k_s, \quad k_{i\mu}\simeq k_{s\mu}, \quad k_{i0}\simeq k_{s0} \; . \tag{50b}$$

The, the relations (49) become, respectively,

$$k_p+2k_i+\frac{2\pi m}{D}=0 \tag{51a}$$

and

$$k_p+\frac{2\pi m}{D}=0 \; . \tag{51b}$$

The numerical calculations of Sec. III are carried out under this hypothesis. As a matter of comparison it is also worthwhile to calculate the scattered field intensity by assuming that the superlattice is infinite rather than semi-infinite; this means that the radiation generated by the polarization propagates into an infinite superlattice on both sides of the polarized region (which still extends over the unit cell $n=0$ to $n=N-1$). In this case the solution in (40) still remains valid beyond the Nth unit cell; on the other hand, the solution in (38), corresponding to the region before the unit cell $n=0$, should be replaced by a Bloch wave propagating along the negative x_3 direction

$$E(n,\mu,x_3^{(n)};t)=(\tilde{A}_{s\mu}e^{ik_{s\mu}x_3^{(n)}}+\tilde{B}_{s\mu}e^{-ik_{s\mu}x_3^{(n)}})e^{-i(nk_sD+\omega_s t)} \; . \tag{52}$$

The coefficients $\tilde{A}_{s\mu},\tilde{B}_{s\mu}$ are known quantities, given by Eqs. (23) where k_s should be replaced by $-k_s$, except for an amplitude $\tilde{E}_s$.

Now, we write again the boundary conditions at the limits of the polarized region; assuming again $N\gg 1$, we find the following results for the amplitudes of the forward and backward scattered fields in the superlattice:

$$\frac{E_s}{E_i}=e^{-ik_sD}\frac{e^{iN\Delta k_- D}-1}{e^{i\Delta k_- D}-1}w \; , \tag{53a}$$

$$\frac{\tilde{E}_s}{E_i}=-e^{ik_sD}\frac{e^{iN\Delta k_+ D}-1}{e^{i\Delta k_+ D}-1}v \; , \tag{53b}$$

where $\Delta k_\pm$ are defined by Eq. (44). A simpler way to obtain the results (53) is to make $r_s=0$, $t_s=1$ in Eqs. (45). The relative intensity of the scattered light can be obtained as in (48),

$$I=\frac{\sin^2(N\,\Delta k_\pm D/2)}{\sin^2(\Delta k_\pm D/2)}\times\begin{cases} v^2 \;\; (\text{backward}) & (54\text{a})\\ w^2 \;\; (\text{forward}) & (54\text{b})\end{cases}$$

and the wave-vector selection rules become

$$k_p+k_i+k_s+\frac{2\pi m}{D}=0 \;\; (\text{backward}) \; , \tag{55a}$$

$$k_p+k_i-k_s+\frac{2\pi m}{D}=0 \;\; (\text{forward}) \; . \tag{55b}$$

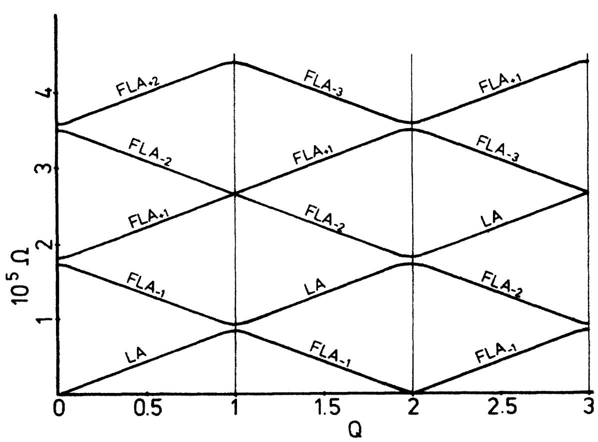

FIG. 2. Frequencies of the excited phonon branches as a function of the reduced scattering wave vector ($Q=qD/\pi$).

The difference between the results in Eqs. (45)–(49) and those in Eqs. (53)–(55) comes from the fact that in the former case the scattered field in the polarized region undergoes reflection and refraction at the surface of the superlattice, while in the latter case the superlattice is an infinite medium. The effects of these wave reflections and transmissions are contained in the factors t_s, t_i [Eqs. (47) and (48)] which affect the absolute intensities of the scattered lights, but disappear if we are only interested in the relative intensities of the folded acoustic phonons at a given scattering wave vector $k_i \pm k_s$.

In the infinite superlattice, one can notice that the backward (forward) scattered light presents peaks at the folded acoustic modes corresponding to the phonon wave vector given by Eq. (55a) [(55b)]. For a semi-infinite superlattice, the light scattered backward into the vacuum still shows peaks for wave vector satisfying the condition (55a) or (49a); however, in the forward scattering there are two series of peaks corresponding to both conditions, Eqs. (55). A similar calculation in the case of a finite superlattice, bounded by air on both sides, may enable one to show that due to the reflection of the scattered light at both ends of the superlattice, both the backward and forward scattered fields contain the two series of peaks given by Eqs. (55).

D. Discussion of a few limiting cases

In previous works[3,8] the intensity of the scattered light was calculated by taking into account the square-wave modulation of photoelastic and/or elastic constants in the superlattice, but assuming that the superlattice behaves like a homogeneous medium as regards the propagation of incident or scattered lights. The incident light in the superlattice is then a plane wave

$$E_i(x_3,t)=E_i e^{i(k_i x_3-\omega_i t)} . \tag{56}$$

The scattering intensity can be written as the square modulus of the Fourier transform of the polarization field:[3,14]

$$I \sim \left| \int_{-\infty}^{+\infty} dx_3 e^{\pm i k_s x_3} P(x_3,t) \right|^2 \tag{57a}$$

or

$$I \sim \left| \int_{-\infty}^{+\infty} dx_3 e^{iqx_3} p(x_3) \frac{\partial u_3(x_3,t)}{\partial x_3} \right|^2 . \tag{57b}$$

Here $P(x_3,t)$ is the polarization field as defined by Eq. (26), $p(x_3)$ is the photoelastic constant, and q is the scattering wave vector ($q=k_i \pm k_s$ in our notation). Let us also recall that we are dealing with anti-Stokes, rather than Stokes polarization. Using Eq. (2) in Eq. (57b)

$$I \sim \sum_m \delta \left[k_p + q + \frac{2\pi m}{D} \right] \left| p_1 k_{p1} \left[\frac{a_1^{(0)}(e^{i(k_{p1}+q)d_1}-1)}{k_{p1}+q} - \frac{b_1^{(0)}(e^{i(-k_{p1}+q)d_1}-1)}{-k_{p1}+q} \right] \right.$$
$$\left. + e^{iqd_1} p_2 k_{p2} \left[\frac{a_2^{(0)}(e^{i(k_{p2}+q)d_2}-1)}{k_{p2}+q} - \frac{b_2^{(0)}(e^{i(-k_{p2}+q)d_2}-1)}{-k_{p2}+q} \right] \right|^2 . \tag{58}$$

Here the quantity inside the square modulus comes from the integration in (57b) over one unit cell, while the Dirac function results from integration over $N \gg 1$ unit cells. In Ref. 8, the authors obtained the scattering intensity from Eq. (57b) but they calculated the elastic displacement field $u_3(x_3,t)$ numerically rather than using its analytic expression (2) leading to the simple closed form relation (58).

The result given by Eq. (58) can be obtained as a limiting case of the general expression (54) by making the assumptions that the two layers in the superlattice are optically identical and described by an effective dielectric constant; in our geometry of scattering this effective value is given by[13,15]

$$\epsilon_e = \frac{d_1\epsilon_1 + d_2\epsilon_2}{D} . \tag{59}$$

We do not present here the detail of this calculation, which is straightforward.

In Sec. III, we give a numerical comparison of the exact and approximate results. In the following we shall introduce additional assumptions which lead to simpler expressions of the scattering intensity.

(a) Let us first assume that there is no acoustic mismatch between the two layers in the superlattice; this means $\rho_1 v_1 = \rho_2 v_2$ or $\rho_1 c_1 = \rho_2 c_2$. With this approximation, the dispersion curve of the phonons (Fig. 1) becomes a straight line whose equation is given by (11) and (12). After some algebra, one finds

$$I \sim \sin^2\left\{\frac{d_1}{D}\left[\frac{\omega_p d_2}{2}\left[\frac{1}{v_1}-\frac{1}{v_2}\right]\mp\pi m\right]\right\}\left|\frac{\dfrac{p_1}{v_1}}{\dfrac{\omega_p d_2}{D}\left[\dfrac{1}{v_1}-\dfrac{1}{v_2}\right]\mp\dfrac{2\pi m}{D}}-\frac{\dfrac{p_2}{v_2}}{\dfrac{\omega_p d_1}{D}\left[\dfrac{1}{v_2}-\dfrac{1}{v_1}\right]\mp\dfrac{2\pi m}{D}}\right|^2 , \quad (60)$$

where m is the folding index which relates the scattering wave vector q to the phonon wave vector k_p by $q+k_p+2\pi m/D=0$ [Eq. (55a)]; the minus or plus sign is to be used in Eq. (60) depending on whether k_p is positive or negative for the corresponding mode.

This expression becomes even simpler if one assumes that the two layers in the superlattice have the same acoustic parameters: $\rho_1=\rho_2$ and $v_1=v_2$. Then, for $m\neq 0$, we directly obtain, from (60),

$$I_m \sim \frac{\sin^2(\pi m/D)}{(\pi m)^2}(p_1-p_2)^2 . \quad (61a)$$

For $m=0$, the expression (60) gives, in the limit $v_1\rightarrow v_2$,

$$I_0 \sim \left[\frac{d_1p_1+d_2p_2}{D}\right]^2 . \quad (61b)$$

In particular, the ratio of the folded acoustic modes to the Brillouin line is given by

$$\frac{I_m}{I_0}=\frac{\sin^2(\pi m/D)}{(\pi m)^2}\frac{(p_1-p_2)^2}{[(d_1p_1+d_2p_2)/D]^2} . \quad (61c)$$

The expressions (61), first derived by Colvard *et al.*,[3] are clearly approximate, as they are not dependent upon the wave vector of the phonon and they also lead to the same intensity for the two components of the FLA doublets, respectively labeled by the indices $+m$ and $-m$. Besides the necessity of having a scattering wave vector q smaller than the size of the Brillouin zone, the approximate validity of the above results also requires that q be in a range where the true dispersion curves (Fig. 1) are well approximated by straight lines.

(b) We now consider the limit of Eq. (58) where the acoustic wavelengths become large compared to the period D ($k_pD \ll 1$, $\omega_pD/v \ll 1$) and the superlattice behaves like an effective homogeneous medium characterized by effective elastic, photoelastic, and dielectric constants. The long-wavelength expansion of Eq. (58) gives, for the intensity of the Brillouin line (which is the only peak in the limit considered),

$$I \sim \frac{p_e^2}{C_e} . \quad (62)$$

This is the expression for a homogeneous medium where the two effective parameters p_e and C_e are defined by

$$\frac{D}{C_e}=\frac{d_1}{C_1}+\frac{d_2}{C_2} \quad (63a)$$

and

$$D\left[\frac{p_e}{C_e}\right]=d_1\frac{p_1}{C_1}+d_2\frac{p_2}{C_2} . \quad (63b)$$

The general expressions of the effective elastic, dielectric, and photoelastic constants as functions of the parameters of the two materials are given in Ref. 15. Equations (63) are two of these relations containing the particular constants we used in our geometry of scattering. Let us recall that the meanings of C and p are, respectively, C_{33} and $\epsilon_{11}^2 p_{1133}$.

III. APPLICATION TO GaAs-AlAs SUPERLATTICES AND GENERAL DISCUSSIONS

In this section we present examples of intensity calculations for the backward scattering in GaAs-AlAs superlattices, using either the exact calculation or different levels of approximations. We also investigate the behavior of the scattering intensity as a function of the relative photoelastic parameter and thickness of the layers.

In Fig. 3, the scattering intensities [Eq. (48)] from the first few folded phonon branches are presented for a GaAs-AlAs superlattice, with $d_{AlAs}/D=0.74$, as functions of the dimensionless scattering wave vector $Q=qD/\pi$. The intensities show drastic variations, especially for Q close to integer values. The Brillouin line LA is the most intense mode for large domains of Q values, except near the boundaries of the successive Brillouin zones. As we shall discuss later, these behaviors are due

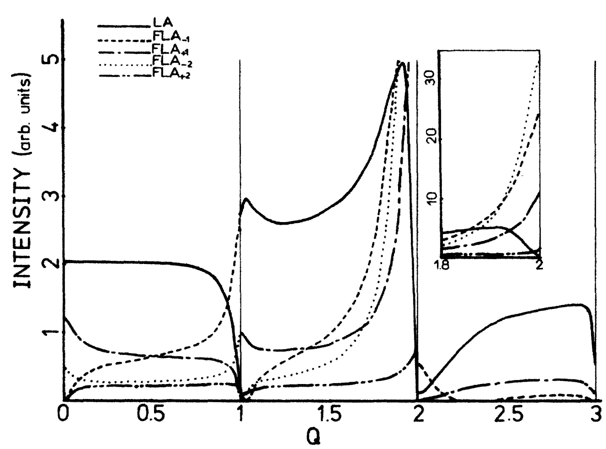

FIG. 3. Intensities of the Brillouin and of the first few folded modes [Eq. (49)] in a GaAs-AlAs superlattice with $d_{AlAs}/D=0.74$, and $p_2/p_1=0.15$. The refractive indexes of GaAs and AlAs are, respectively, $n_1=4.395$ and $n_2=3.37$ (corresponding to $\lambda=4880$ Å). For Q close to the boundary to the second Brillouin zone, several modes becomes very intense, as shown in the inset.

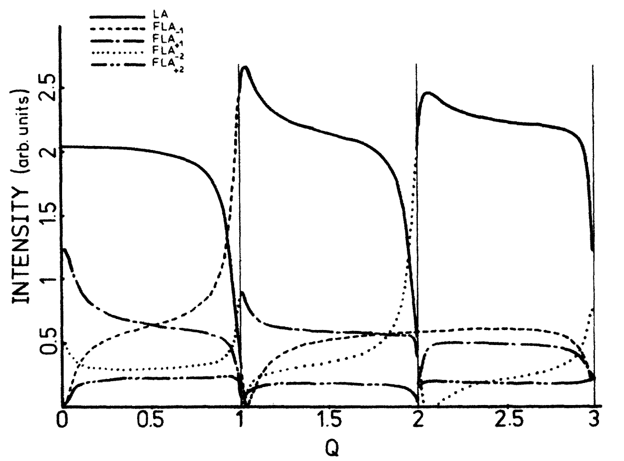

FIG. 4. Same as in Fig. 3 but neglecting the electromagnetic mismatch between the two layers.

to the complex interferences resulting from the reflections of the acoustic and electromagnetic waves at the interfaces in the superlattice. Figure 4 gives the scattering intensities from the folded modes as functions of Q when one assumes that the refractive indices of the two media in the superlattice are identical ($n_1=n_2$) and equal to an effective value n_e [see Eq. (59)]; this means that there is no reflection of the electromagnetic waves at the interfaces. In comparison with Fig. 3, noticeable differences occur for $Q>1$, and more particularly near $Q\simeq2$, which corresponds to the Bragg condition for the light. Thus for scattering wave vectors exceeding the first Brillouin zone, the effect of the electromagnetic wave reflections at the interfaces cannot be neglected.

In a further approximation one can also assume that the two media have identical elastic parameters; this means that the elastic waves in the superlattice are approximated by plane waves. The intensities of the scattering light from the folded branches are then independent of the Q wave vector and identical for the $(FLA)_m$ and $(FLA)_{-m}$ branches [see Eqs. (61)]. Figure 5 gives a comparison of the $(FLA)_{\pm1}$ intensity in this approximation with the exact results; the intensities are calculated with respect to that of the Brillouin line, which is normalized to one. The most important deviations between the two sets of results occur for Q close to integer values.

To explain these behaviors, let us first consider the case where the acoustic and electromagnetic waves in the superlattice are approximated by plane waves, in other words, the acoustic and optic parameters of the two media are replaced by effective parameters. Thus the polarization produced by the photoelastic effect [see Eq. (26)] has a phase factor $e^{i(k_p+k_i)x_3}$, while the phase factor of the scattered light is $e^{-ik_sx_3}$ (for backward scattering). From Eq. (49a) we can see that these two factors are equal for the Brillouin mode ($m=0$), thus the elementary waves generated at different points of the superlattice are in phase and give rise to constructive interference. This can also be seen from Eq. (57a), where the phase factor in the integrand $e^{i(k_p+k_i+k_s)x_3}$ becomes a constant (equal to 1). But for the folded mode ($m\neq0$), this phase factor becomes $e^{-i2\pi mx_3/D}$ and the elementary waves generated in different points of a unit cell are not totally constructive

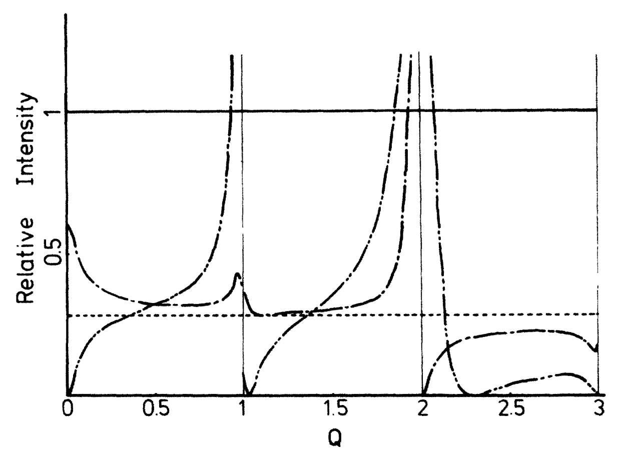

FIG. 5. Comparison of the relative intensities $I((FLA)_{\pm1})/I(LA)$ obtained by our calculation [—·—·—, $(FLA)_1$; —··—, $(FLA)_{-1}$] and from ref. 3 [— — —, $(FLA)_{\pm1}$]. The parameters of the superlattice are the same as in Fig. 3.

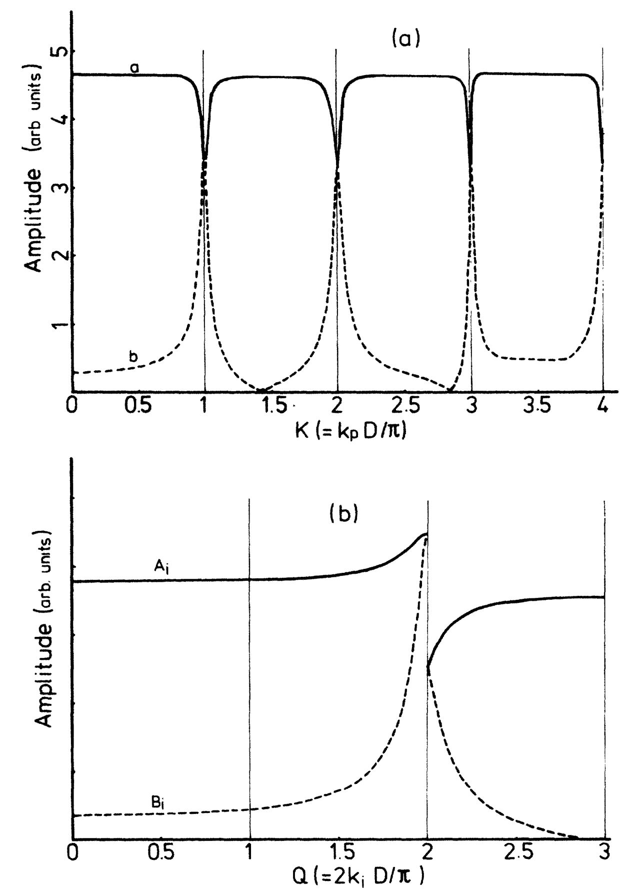

FIG. 6. Amplitudes of the acoustic (a) and incident electromagnetic (b) waves in the GaAs layers. The solid and dashed lines correspond, respectively, to the components of the wave propagating in the positive and negative x_3 direction. The amplitudes in the AlAs layers have similar behaviors. The parameters of the superlattice are the same as in Fig. 3.

(however, the ones generated in successive unit cells remain constructive). Therefore the intensities of the folded modes may be much smaller than that of the Brillouin mode and depend strongly on the structure of the unit cell.

In a real superlattice, where the acoustic and optic parameters of the layers are different, the polarization inside each medium contains four terms [Eq. (27)]:

$$a_\mu^{(0)} A_{i\mu}^{(0)} e^{i(k_{p\mu}+k_{i\mu})x_3}, \quad a_\mu^{(0)} B_{i\mu}^{(0)} e^{i(k_{p\mu}-k_{i\mu})x_3},$$

$$b_\mu^{(0)} A_{i\mu}^{(0)} e^{i(-k_{p\mu}+k_{i\mu})x_3}, \quad b_\mu^{(0)} B_{i\mu}^{(0)} e^{-i(k_{p\mu}+k_{i\mu})x_3},$$

instead of one in the case of plane waves, due to the acoustic or electromagnetic wave reflections at the interfaces. The moduli of the amplitudes $a^{(0)},b^{(0)}$ ($A_i^{(0)},B_i^{(0)}$) in GaAs layers are represented in Fig. 6(a) [Fig. 6(b)] as a function of $K=k_pD/\pi$ ($Q=qD/\pi=2k_iD/\pi$). One can notice that, except near the Bragg condition $k_p=l\pi/D$ ($k_i=l\pi/D$), one of the two coefficients $a^{(0)},b^{(0)}$ ($A_i^{(0)},B_i^{(0)}$) is much smaller than the other; so only one among the four terms appearing in the polarization plays a dominant role. Furthermore, if the acoustic and optic properties of the layers are close to one another, both wave vectors $k_{p\mu}$ ($k_{i\mu}$) become comparable to k_p (k_i) and one recovers the approximation in which the Bloch waves can be replaced by plane waves. However, for Q close to integer (even integer) values, the coefficients $a^{(0)},b^{(0)}$ ($A_i^{(0)},B_i^{(0)}$) become of the same order; in this case two or even all of the four terms in the polarization are important and affect the scattering intensity. The contribution of the four terms to the scattered light can be constructive or destructive, thus the intensities of the modes increase or decrease drastically and certain modes becomes more intense than the Brillouin line.

Figures 7 and 8 present the influence of the relative thickness of the layers in the superlattice on the scattering intensities of the folded modes. In Fig. 7, the thicknesses of the GaAs and AlAs layers are assumed to be the same. One can notice a different behavior of the $(\mathrm{FLA})_m$ intensities compared to those in Fig. 3; besides, the folded branches with even order indices are less intense. These last modes have vanishing intensities except

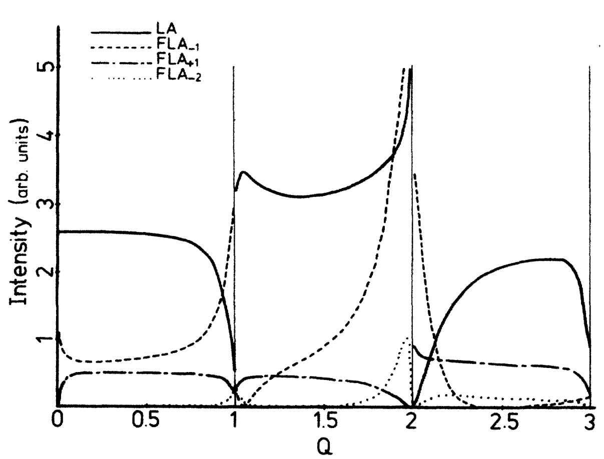

FIG. 7. Same as in Fig. 3 but in a superlattice with $d_1=d_2=D/2$.

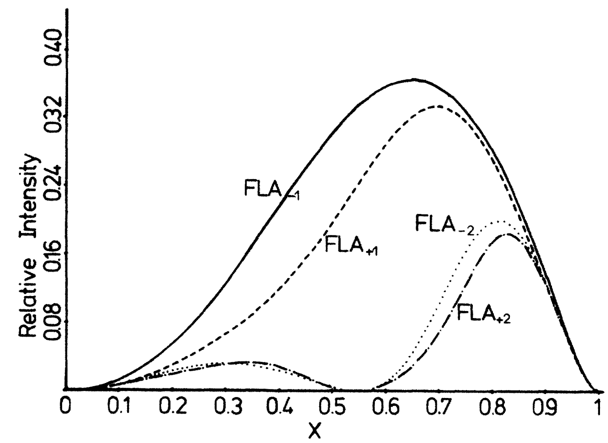

FIG. 8. Variations of the relative intensities $I((\mathrm{FLA})_m)/I(\mathrm{LA})$ with the relative thickness of the layers $x=d_{\mathrm{AlAs}}/D$. The period of the superlattice is $D=186$ Å and the wavelength of the light $\lambda=4880$ Å; the other parameters are those of Fig. 3.

when Q is close to integer values; this is consistent with the results of Colvard *et al.*[3] [see Eqs. (61)] where, for $d_1=d_2=D/2$, the intensities of the folding branches with even indices are zero.

The dependence of the intensities on the relative thickness of the layers is given in Fig. 8, where the period of the superlattice is $D=186$ Å and the wavelength of the light $\lambda=4880$ Å. Here the intensity of the Brillouin line is normalized to one. As the folding index $|m|$ increases, the curves show more oscillations while the general tendency for the intensities is to decrease. Let us also notice that the intensities of $(\mathrm{FLA})_{\pm 2}$ vanish at a value of d_2/D which is slightly greater than $\frac{1}{2}$ (see the discussion of the preceding paragraph); this difference, which is due to the deviations of the waves in the superlattice from plane waves, is a consequence of the modulation of acoustic and optic properties of the superlattice.

Finally, the variations of the intensities of the $(\mathrm{FLA})_{\pm 1}$ modes compared to the Brillouin mode as a function of

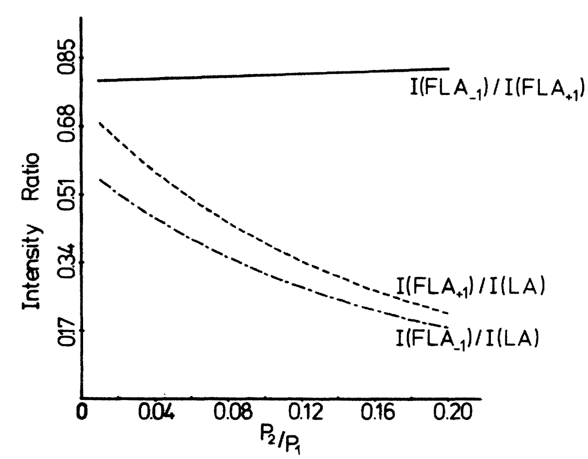

FIG. 9. Variations of relative intensities $I((\mathrm{FLA})_{\pm 1})/I(\mathrm{LA})$ and $I((\mathrm{FLA})_{-1})/I((\mathrm{FLA})_1)$ as a function of the relative photoelastic parameter. The other parameters are $D=421$ Å, $d_{\mathrm{AlAs}}/D=0.73$, and $\lambda=4880$ Å.

the relative photoelastic parameter p_2/p_1 are sketched in Fig. 9; here the period of the superlattice is $D=421$ Å, $d_2/D=0.73$, and the wavelength of the light $\lambda=4880$ Å. By increasing p_2/p_1 from 0, the relative intensities $I((\mathrm{FLA})_{\pm 1})/I(\mathrm{LA})$ significantly decrease while the ratio $I((\mathrm{FLA})_{-1})/I((\mathrm{FLA})_{+1})$ remains almost constant. Thus the measurements of the folded mode intensities with respect to the Brillouin lines are necessary to obtain a good determination of the ratio P_2/P_1. This intensity behavior is exploited in Ref. 9 to characterize the photoelastic properties of GaAs/AlAs.

IV. CONCLUSIONS

In this paper we have calculated the light scattering intensity by longitudinal-acoustic phonons propagating along the axis of a superlattice. An analytic approach has been used and the results of the previous works which contain some simplifying assumptions have also been derived. To calculate the intensities of the Brillouin and the folded modes exactly and to determine their dependence on the scattering wave vector, we showed that it is necessary to take into account the modulation not only of photoelastic and acoustic but also of optic properties of the superlattice, especially for a scattering wave vector q greater than the size π/D of the Brillouin zone. The measurements of these intensities and in particular the ratios of the FLA intensities to the Brillouin intensity enable one to obtain useful information about the relative thickness and the photoelastic parameter of the layers.

The calculation was carried out by assuming that the number of polarized layers which contribute to the radiation field goes to infinity. If this number if not very large, the peaks in the scattered field are broadened instead of being delta functions. This effect is superimposed on other contributions to the broadening of the peaks, resulting from acoustic or optic absorption and the presence of defects.[16] Finally let us point out that our calculation can be extended to problems where different mechanisms of coupling between the light and the phonons or other excitations are involved.

[1] L. Colvard, R. Merlin, M. V. Klein, and A. C. Gossard, Phys. Rev. Lett. **45**, 298 (1980).

[2] J. Sapriel, J. C. Michel, J. C. Toledano, R. Vacher, J. Kervarec, and R. Regreny, Phys. Rev. B **28**, 2007 (1983).

[3] C. Colvard, T. A. Gant, M. V. Klein, R. Merlin, R. Fisher, H. Morkoc, and A. C. Gossard, Phys. Rev. B **31**, 2080 (1985).

[4] B. Jusserand, D. Paquet, A. Regreny, and J. Kervarec, Solid State Commun. **48**, 499 (1983).

[5] H. Brugger, G. Abstreiter, H. Jorke, H. J. Herzog, and E. Kasper, Phys. Rev. B **33**, 5928 (1986).

[6] D. J. Lockwood, M. W. C. Dharma-Wardana, J. M. Baribeau, and D. C. Houghton, Phys. Rev. B **35**, 2243 (1987).

[7] M. Babiker, D. R. Tilley, E. L. Albuquerque, and C. E. T. Gonçalves da Silva, J. Phys. C **18**, 1269 (1985).

[8] B. Jusserand, D. Paquet, F. Mollot, F. Alexandre, and G. Le Roux, Phys. Rev. B **35**, 2808 (1987).

[9] J. Sapriel, J. He, B. Djafari-Rouhani, R. Azoulay, and F. Mollot, following paper, Phys. Rev. B **37**, 4099 (1988).

[10] F. Abélès, Ann. Phys. (Paris) **5**, 596 (1950).

[11] P. Yeh, A. Yariv, and C. S. Hong, J. Opt. Soc. Am. **67**, 423 (1977).

[12] R. E. Camley, B. Djafari-Rouhani, L. Dobrzynski, and A. A. Maradudin, Phys. Rev. B **27**, 731 (1983); B. Djafari-Rouhani, L. Dobrzynski, O. Hardouin Duparc, R. E. Camley, and A. A. Maradudin, *ibid.* **28**, 1711 (1983).

[13] S. M. Rytov, Akust. Zh. **2**, 71 (1956) [Sov. Phys.—Acoust. **2**, 68 (1956)]; see also L. M. Brekhovskikh, *Waves in Layered Media* (Academic, New York, 1960).

[14] W. Hayes and R. Loudon, *Scattering of Light by Crystals* (Wiley, New York, 1978).

[15] B. Djafari-Rouhani and J. Sapriel, Phys. Rev. B **34**, 7114 (1986).

[16] J. Sapriel, J. He, J. Chavignon, F. Alexandre, R. Azoulay, G. Le Roux, J. Burgeat, and R. Vacher, in *Proceedings of the European Materials Research Society, Strasbourg, June 1986*, edited by P. A. Glasow, Y. I. Nissim, J.-P. Noblanc, and J. Speight (Les Editions de Physique, Paris, 1986), p. 267.